Stony Brook University

Electrospun hydroxyapatite incorporated biocomposite scaffolds for tissue engineering

A Thesis presented

by

Koushik Ramachandran

to

The Graduate School

in Partial Fulfillment of the

Requirements

for the Degree of

Master of Science

In

Materials Science and Engineering

Stony Brook University

December 2007

Stony Brook University

The Graduate School

Koushik Ramachandran

We, the thesis committee for the above candidate for the

Master of Science degree, hereby recommend

acceptance of this thesis.

Dr. Pelagia-Irene (Perena) Gouma, Thesis Advisor, Associate Professor
Department of Materials Science and Engineering

Dr. Dilip Gersappe, Associate Professor
Department of Materials Science and Engineering

Dr. Andrew Gouldstone, Assistant Professor
Department of Materials Science and Engineering

This thesis is accepted by the Graduate School

Lawrence Martin
Dean of the Graduate School

Abstract of the Thesis

Electrospun hydroxyapatite incorporated biocomposite scaffolds for tissue engineering

by

Koushik Ramachandran

Master of Science

In

Materials Science and Engineering

Stony Brook University

2007

This work is aimed at exploring the feasibility of cellulose acetate and its hydroxyapatite incorporated nanocomposite hybrid as scaffold materials for bone tissue engineering. The fibrous scaffolds were fabricated using electrospinning and were characterized using electron microscopy. Human osteoblasts (SaOS2) were cultured and seeded on these scaffolds. MTS assay and PicoGreen assay were conducted on day 1 and day 3 of cell seeding process to determine the cellular metabolic activity and quantitation of double-stranded DNA. The results obtained indicated a significant increase in cell growth, confirming that both the scaffolds actively support osteoblast growth. Cells were fixed on the scaffolds for characterization using scanning electron microscopy and fluorescence microscopy. Characterization studies determined the morphology of cell attachment on the various types of scaffolds. The use of hydroxyapatite nanoaggregates appear to enhance cell attachment and possibly influence cell differentiation. These fibrous nanocomposite scaffolds are promising materials for bone tissue engineering.

Table of contents

List of figures

List of tables

ACKNOWLEDGEMENT

I would like to thank my advisor Professor Perena Gouma, for the guidance, encouragement and support I received through out the course of my work.

I wish to thank Dr. Peter Perrotta, West Virginia University for making this project possible and EPA, STAR Project for the funding support. I would like to thank Dr. Ronald Zuckermann, Melike Firat and Michael Connolly at the Molecular Foundry, Lawrence Berkeley National Laboratory for their help with the cell culture experiments. I would also like to thank Dr. Jim Quinn for his help in carrying out the SEM experiments. I am grateful to Dr. Michael Hadjiargyrou for his advice and help in using the fluorescence microscopy. I wish to thank Prof. Dilip Gersappe and Prof. Andrew Gouldstone for being on my thesis committee. I would like to extend my thanks to my group members Krithika, Lisheng and Aisha for their help and support in carrying out my work.

Finally, I thank my mom, dad and my brother for being there for me at all times.

1. INTRODUCTION

1.1 Bone tissue engineering

Langer and Vacanti [1] have defined tissue engineering as "an interdisciplinary field of research that applies the principle of biology and engineering toward the development of biological substitutes that restore, maintain or improve tissue function". Bone tissue engineering has emerged as a subject of significant interest in the past decade as most of the injuries related to bone are unrecoverable and changes in the bone structure due to an injury dramatically alters ones' body equilibrium [2]. There are about 1 million cases of skeletal defect a year that require bone-graft procedures for reconstruction [3]. The need for improved treatment of the defects has led to the development of several natural and synthetic materials [1]. Various techniques have been employed to reconstruct bone defects. The techniques currently available for reconstruction of bone defects are by using autologous bone grafts (from the patient), allogenic bone grafts (from a donor) and various biomaterials. Autologous bone transplant has remained as the golden standard for treatment of bone defects. Although a successful procedure, this technique is limited by material availability. Allogenic bone graft technique, an alternative that involves bone transplant from a donor, may introduce immune rejection and pathogen transfer [1, 2].

Cell-based approach for bone grafting that makes use of scaffolds fabricated from natural or synthetic biomaterials including metals, ceramics, polymers and composites has been recognized as a promising technique to overcome the drawbacks of autologous and allogenic bone-graft techniques [1-4]. In cell-based approach, three dimensional

scaffolds or bioscaffolds that function as carrier for the cells are used [4]. The scaffolds should possess certain key properties to serve as a temporary matrix for bone growth.

Some of the properties that have been identified as essential are biocompatibility, porosity, pore size, surface property, osteoinductivity, biodegradability and mechanical properties. Biocompatibility is important because the scaffolds should not induce an immune response. Porosity and pore size are important for cell growth, nutrient transfer and oxygen transport. Osteoinductivity is a key requirement for stimulating the cells to undergo the osteoinductive path. Mechanical properties and biodegradability are required for load bearing and allowing for total regeneration of bone respectively [4-7].

1.1.1 Biomaterials for bone tissue engineering scaffolds

The first and important step towards bone tissue engineering technique is choosing the appropriate material which satisfies all the criteria as already discussed. Several materials have been identified and tested as scaffold materials. Biodegradability being one of the most important requirements, limits the choice of materials to a few ceramics and polymers [4].

Several natural and synthetic ceramics have been used in the field of bone engineering. Ceramics are considered as ideal materials because of their osteoinductive properties, the ability to induce bone formation. Synthetic ceramics such as β-tricalcium phosphate and synthetic hydroxyapatite (HA) have been used. Ceramics have been used in several works [8-12] and have been shown to provide good support for bone regeneration. One of the major disadvantages of ceramic material is its brittleness, leading to poor mechanical stability. High degradation rate can also lead to a problem of increased concentrations of Ca and P, which may be detrimental to bone growth.

Natural and synthetic biodegradable polymers have been evaluated as scaffold materials to overcome the disadvantages of ceramic materials. Biodegradable polymers are those that can break down due to macromolecular degradation by attack of biological elements [7]. Some of the natural polymers used thus far include collagen, fibrinogen, starch and poly(hydroxybutyrate) [13-16]. The advantages offered by natural polymers are good bioactivity and chemical versatility [2]. The other advantage of utilizing natural polymers includes their low cost attributed to abundant availability [14]. Collagen, a natural polymer has been evaluated as bone tissue engineering scaffold by seeding collagen films and scaffolds with human mesenchymal stem cells. A high amount of DNA was observed in slowly degrading collagen constructs, suggesting the ability to control osteogenesis [17]. Cellulose acetate (CA), another natural polymer and a plentiful organic compound found in the higher plants' cell walls [18], can be easily molded or drawn into fibers for use in various applications. Cellulose based materials allow better control over scaffold design due to their low water solubility [19].

Synthetic biodegradable polymers are more recently used in the biomedical engineering field. Poly(α-hydroxy acids) such as lactic acid and glycolic acid are widely used owing to their degradation properties [20-22]. Poly(ε-caprolactone) has been used as scaffolds and have also been blended with other materials to improve mechanical and biological properties [23]. Poly(carbonate) showed good biocompatibility when it was tested as a implant in a bone canine chamber model [24]. Certain poly(phosphazenes) and poly(anhydrides) have also been used as scaffolds owing to their good degradability and support for bone regeneration [25-26].

1.1.2 Techniques for synthesizing tissue engineering scaffolds

Solvent casting was first described by Mikos et al. [20] to prepare highly porous biodegradable polymer membranes. The process involved the casting of polymer/salt composite membranes followed by the dissolution of the salt. Vibration was used during solvent dissolution and evaporation in this technique. It was suggested that this technique was capable of producing scaffolds with tunable porosity and desired crystallinity.

Phase Inversion is similar to solvent casting technique, the main difference being instead of allowing the solvent to evaporate; the film is placed in water resulting in phase separation. PLGA scaffolds were prepared by this technique and were shown to support osteoblast-like cells growth. Mechanical properties of the scaffolds obtained are not ideal for scaffolds. This is one of the main disadvantages of this technique [27].

Melt Molding is used to produce scaffolds with high porosity. This technique involves mixing the polymer with a porogen and then the mixture is loaded into a mold. It is then heated and the porogen is removed by dissolution to make three dimensional scaffolds with high porosity [2]. One of the major drawbacks of this technique is the difficulty in controlling pore distribution. Oh et al. [28] have fabricated porous PLGA/PVA composites using this technique and have evaluated the potential to restore skull defects.

Fiber bonding involves knitting or weaving of individual fibers to fabricate three dimensional scaffolds with variable pore size. Some of the drawbacks of this technique are the lack of control of porosity and pore size. Solvent residues due to immiscibility might harm cells and organs [2].

High pressure processing is a novel technique suggested for fabricating macroporous sponges of biodegradable polymers without the use of organic solvents. Mooney et al. [29] have employed this technique to fabricate poly (D,L-lactic-co-glycolic acid) by saturating them with high pressure CO_2 and then by rapidly reducing the gas pressure to atmospheric levels. These porous sponges have been suggested as ideal candidates for tissue engineering. The process has a few disadvantages such as, low mechanical properties and closed pore structure [2].

Three-dimensional printing (3DP) is a technique that makes use of inkjet technology to produce scaffolds from powders. Scaffolds with different morphology and different materials have been fabricated by this technique. Lee et al. [30] have employed an indirect three dimensional printing technique to fabricate PLGA scaffolds to overcome the limitation of the direct method. Limited layer thickness is one of the major disadvantages of this technique.

Freeze-drying process has been used to prepare hybrid collagen-gelatin polymer networks by Mao et al. [31] by utilizing ice microparticles as porogen. This process depends on thermally induced phase separation. Precise control of parameters is required to fabricate the scaffolds.

Electrospinning, invented by Formhals [32] in 1934 to fabricate fibrous structures of polymers by the application of a high voltage to a viscous polymeric based solution, has recently emerged as a leading technique to fabricate fibrous structures for tissue engineering [33-35] as the process has the unique capability to fabricate three-dimensional scaffolds that can mimic the extracellular matrix (ECM) with tunable porosity and morphology [35]. Electrospun fibers have various diameters ranging

downward from 5 µm to 0.05 µm. The small diameter of the fibers provides high surface area to volume ratio making it suitable for scaffolds for biomedical applications [36]. Electrospinning has emerged as a promising one-step technique to fabricate scaffolds for bone tissue engineering.

Most of these techniques described do not have the capability to produce three dimensional scaffolds with controlled amount of porosity and pore size in a single step. Electrospinning, however a remarkable nanomanufacturing technique has the ability to produce three dimensional biomimicking scaffolds with layered configuration with complex pore structures and controlled pore size [35].

1.2 Electrospinning

Synthetic fibers of polymers have been produced by employing conventional processes such as melt spinning, dry spinning or wet spinning [36]. These processes depend on mechanical forces and have practical limitations such as the inability to produce three dimensional fibrous structures with very fine diameters. Electrospinning or Electrostatic fiber spinning is a novel technique for producing fibers through the action of electrostatic forces [36]. Conventional spinning techniques are limited by their inability to produce fiber diameters less than 2 µm robustly. The limitations of conventional fiber spinning technique are overcome with the use of an electric field. The liquid jet emerging from an orifice can be extended by the use of an electric field to enforce its controlled winding. This process is called electrospinning. Electrospinning process results in decreased diameter of the fibers several orders of magnitude, in the order of hundreds to tens of nanometers [37].

Electrospinning has been gaining increased importance in the field of tissue engineering. The electrospinning technique was discovered nearly 100 years ago [38] and the first patent was issued to Formhals in 1934 [32]. This technique uses electrical forces to produce fibers of nanoscale diameters. The principle of the process is, as the solution emerges from the orifice, and the external electric force overcomes the surface tension of the drop, the solution is ejected as electrically charged jets and shoots towards the oppositely charged electrode. As it reaches the collector, it gets neutralized and collects as dry fibers [37].

Larrondo and Manley revived the technique by using a model fluid to analyze the nature of the streamlines and magnitude of the stream velocities. The drop deformation was measured as a function of intensity and frequency using polymer melts of nylon and polyethylene [39]. Since then, several polymers have been electrospun ranging from few nanometers to micrometers [40-43]. The large surface area to volume ratio, superior mechanical performance and versatility in design has made the technique important for many applications such as composites, biomedicine including tissue engineering, implants, wound dressing membranes and drug delivery [44]. The process also has the versatility to produce non-woven composites of a variety of polymers, fibers and particles.

Dzenis has identified some of the major breakthroughs recently in this area. First is the alignment of fibers. Alignment of nanofibers have the ability to revolutionize the applications of nanofibers, the processes developed thus far show promise in nanofiber manufacturing and assembly. The second breakthrough in electrospinning was the production of continuous ceramic fibers using sol-gel chemistry. The synthesis of nanocomposite fibers is one of the greatest breakthroughs where small particles can be

added to the polymer solution or encapsulated in dry nanofibers. Nonwoven mats can be fabricated by adding soluble drugs, bacterial agents and metal oxide sol gel solutions into polymer solutions [37].

1.2.1 Equipment and Technique

Formhals [31] invented the electrospinning process in 1934 which is shown in figure 1. The polymer solution was discharged using a high electric field from an electrode of negative polarity towards the movable electrode that was at a positive polarity, when a potential difference of 57 kV was applied between the two electrodes. A stripping device was used to remove the fibers. The major drawback was the difficulty involved in removing the fibers adhered to the moving parts. Figure 1 shows the schematic of the apparatus patented in 1934.

Simons [45] patented a process in 1964 for producing a patterned non-woven fabric by collecting it on a segmented receiver consisting of two sets. There was a potential difference between the two receiving sets that resulted in high and low density of fibers. A methyl ethyl ketone solution of polyurethane was employed for electrospinning the fibers. Isakoff [46] patented a process to collect filamentary webs of polymeric sheets on a grounded mobile surface.

Fine et al. [47] designed an electrically charged cup like spinneret containing the thermoplastic solution, which rose to the edge of the cup and into the ambient air by centrifugal force. The jet is formed by an applied voltage and is directed to a ground aluminum screen driven slowly around roller belts. The combination of centrifugal and electrostatic force resulted in high strength fibers. Guignard [48-49] replaced the molten

cup used by Fine et al. [47] with a mobile belt for carrying the charged polymer. As the belt approaches the grounded belt, several jets form and gets collected on the screen.

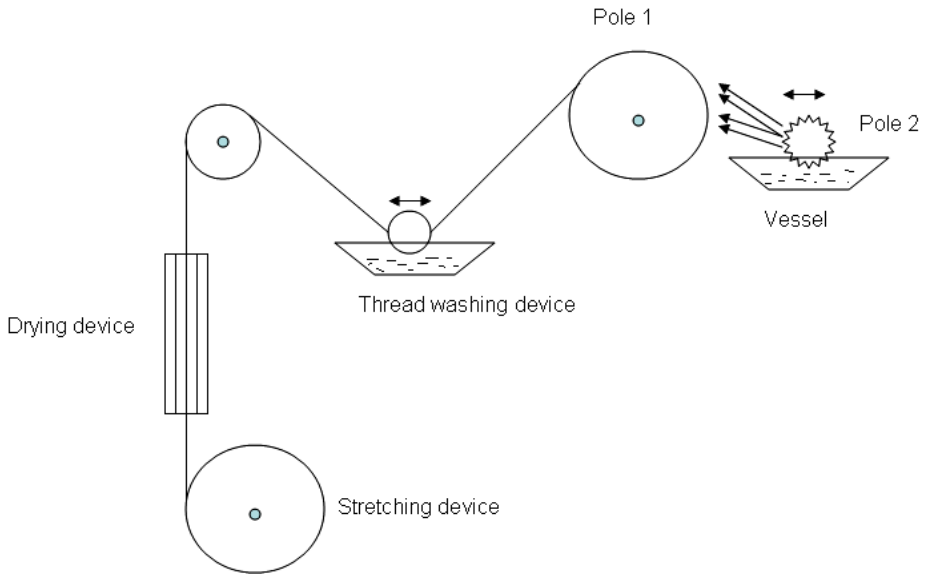

Figure 1 Schematic of the electrospinning apparatus (adapted from [31])

Martin and Derek [50-51] electrospun multicomponent fibers from a single syringe and also demonstrated the possibility of electrospinning solutions of different compositional blends from multiple syringes on stationary or mobile collectors. Bornat [52] devised a method for electrospinning different solutions by placing the syringes in front of a rotating cylindrical metal collector. The syringes were ground and a voltage of -50 kV was applied to the collector. Solidified polymer filaments of poly(ethylene oxide) and poly(tetrafluoroethylene) formed by this method were suggested as blood vessels and urinary ducts.

Simm et al. [53] invented a process to fabricate a composite filter of cellulose fleece covered with a layer of polystyrene. A solution of polystyrene in methylene chloride was electrospun from an annular electrode onto two equidistant collector

electrodes that was covered with a layer of cellulose fibers produced by conventional spinning process.

A typical modern electrospinning setup consists of a programmable syringe pump, a high voltage power supply, precision tip stainless needle and a collector screen. The volume to be electrospun and the flow rate can be programmed in the panel of the syringe pump. During the process, the polymer solution is ejected out of the needle tip under the influence of an electric field as high as 30 kV. The electrostatic charges break up the liquid droplet leading to formation of jets. The jet is extended under the electric field to form a continuous fiber. Before it reaches the collector, the solvent evaporates or solidifies. The fibers are collected on the collector screen as non-woven mats. A conventional electrospinning setup is shown in figure 2.

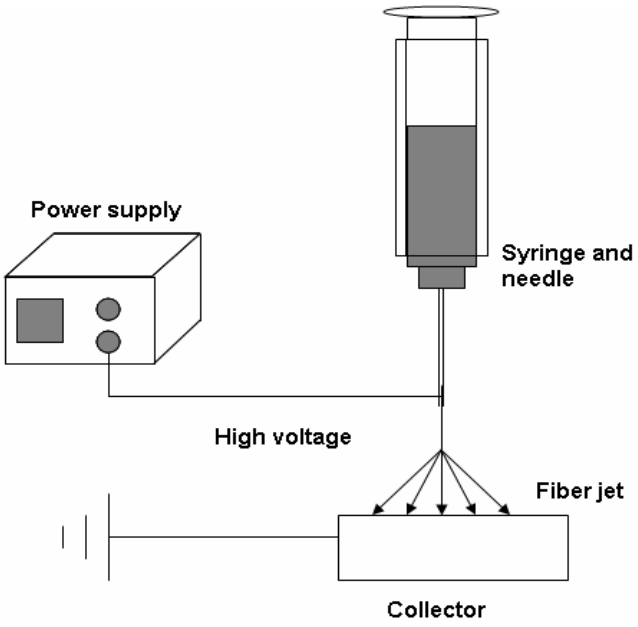

Figure 2 Modern electrospinning setup

1.2.2 Electrospinning process parameters

The morphology of the electrospun fibers depend on a variety of system and process related parameters. Some of the key parameters that affect the fibers are described below [54, 55]

System parameters

1. Solution/melt viscosity
2. Solution concentration
3. Conductivity
4. Surface tension of the fluid
5. Molecular weight of the polymeric precursor
6. Molecular weight distribution in the polymer
7. Topology (branching/linearity) of the polymer
8. Net charge density of the solution

Process Parameters:

1. Strength of the applied voltage
2. Solution flow rate
3. Distance between the dispensing needle tip and the collector plate
4. Chamber temperature and humidity
5. Ambient environment (air versus inert gas or vacuum)
6. Collector plate status – stationary or mobile
7. Internal diameter of the needle

A decrease in volume charge density with increasing flow rate and a decrease in surface charge density with applied voltage was observed for several polymers such as

poly(ethylene)oxide (PEO), poly(acrylic acid) (PAA), poly(vinylacetate) (PVA), polyurethane (PU) , and poly(caprolactone) (PCL) solutions [54, 55]. Deitzel et al. [55] have comprehensively studied the effect of processing parameters on the morphology of electrospun fibers. It was found that the diameter of PEO fibers increased with solution concentration according to a power law relationship. The strength of the electric field must overcome the force of surface tension at the tip of the needle. An increase in voltage leads to a decrease in stability of the originating jet resulting in bead defects in the electrospun fibers. Solution parameters such as viscosity, concentration and surface tension were also found to strongly influence the fiber morphology.

The concentration and molecular weight of the polymer solution are the two main factors that influence polymer chain entanglement. Below the critical concentration required to obtain fibers, no chain entanglement is observed. When the concentration equals the critical concentration, chain entanglement occurrence begins. This critical value is different for different polymers. Shenoy et al. [56] have described the critical concentration for different types of polymer solutions. It was also shown that the diameter of the fibers increased with the increase in concentration of the polymer solution. A high concentration of the polymer solution leads to instability in the process. Table 1 describes the critical values of polymer concentration for fiber initiation.

Solution viscosity, net charge density and surface tension of the polymer solution largely influence the formation of fiber beads. High viscosity and net charge density will reduce the amount of beads. High surface tension will increase the amount of beads [56].

Mckee et al. [57] have studied the effect of process parameters and system parameters on morphology of the fibers. It was found that decreasing the distance

between the needle and the collector resulted in the formation of beads. An increase in voltage was observed to decrease the fiber diameter. The viscosity of the solution should be high enough to form a semi-stable fluid globule at the needle tip and low enough to cause motion in the electric field.

Table 1 Polymer concentration for different polymer/solvent systems (adapated from [56])

Polymer/Solvent	Molecular weight ($x10^3$ g/mol)	Polymer concentration (wt%)	
		Fiber initiation (fibers and beads)	Fibers only
PS/THF	190	18	30-35
PDLA/DMF	109	<20	30-35
PLLA/DCM	670	<1	3
PLLA/$CHCl_3$	670	-	<4.1
PLLA/$C_2H_2Cl_4$	670	<3	>4
PEO/ H_2O	400	NR	4
PEO/ H_2O	2000	NR	<2
PVP/EtOH	1300	3	7-9

1.3 Applications of electrospinning in tissue engineering

The goal is to fabricate a three dimensional scaffold using a biomaterial to provide support and guide cell differentiation and proliferation into new tissues. The

scaffolds have to be porous in order to allow cell growth in to the matrix. Porosity is an important requirement for a scaffold because of the need for nutrient delivery, gas exchanges and removal of waste products [14]

An ideal tissue engineering scaffold combines both mechanical and biological functionality required for cell growth. Mechanical functionality is dependent on the biomaterial chosen and biological functionality is governed by biological signals, surrounding cells and extracellular matrix (ECM). ECM molecules are reported to regulate cellular activity [33]. In view of trying to replicate the ECM consisting of multilayered fibrous and porous architecture, electrospinning has emerged as a successful manufacturing technique for tissue engineering. Several studies have been conducted to explore the feasibility of electrospun threads as matrix for tissue growth.

The polymeric backbone of the scaffold can either be a first responder for initiation and propagation of a joining process or as an active participating scaffold that helps in cell attachment, carrying the nutrients and inorganic components to form or repair a tissue. The scaffolds are expected to aid cell behaviors such as migration, proliferation, differentiation, maintenance of the visible characteristics of the microorganism resulting from the interaction between its genetic makeup and the environment, and the ultimate cell death. These are achieved through continuous cell-matrix interactions [53-59].

A fibrous structure fabricated by electrospinning is found to possess features that bear morphological similarity to ECM. High porosity and good mechanical stability are features of the electrospun scaffold that makes it ideal as an engineering scaffold [33].

1.3.1 Electrospun biomaterials for bone tissue engineering

Several natural and synthetic polymers have been utilized for bone tissue engineering. Some of the materials that have been electrospun and used as bone scaffolds in the recent times have been discussed in this section.

Shih et al. [60] have electrospun type I collagen nanofibers and evaluated it as a bioscaffolds by examining the morphology, motility and differentiation of human bone marrow-derived mesenchymal stem cells (MSCs). It has been reported that type I collagen nanofibers support the growth of MSCs and therefore serves to facilitate bone formation. Collagen has also been used with electrospun nanoscale bioactive glass fibers for bone regeneration. These nanocomposites have shown favorable osteoblast growth [61]. Polycaprolactone-collagen composite nanofibrous membrane has also been electrospun for tissue engineering applications [62].

Yoshimoto et al. [63] have electrospun microporous, non-woven poly(ε-caprolactone) (PCL) scaffolds. Fibers down to nanoscale diameters were produced and were used as a scaffold for mesenchymal stem cells (MSCs) derived from bone marrow. Cells cultured, expanded and seeded on these scaffolds were found to penetrate the matrix and produce extracellular matrix in 1 week. It was concluded that these electrospun matrix is ideal for mineralization and production of type I collagen. Baker et al. [64] have studied the effect of nanofiber alignment on cell proliferation behavior on electrospun poly(ε-caprolactone) (PCL) scaffolds. It was concluded that aligned fibers were superior in terms of mechanical properties and serve as a pattern for guided growth compared to non aligned fibers. Nanofibers of PCL/$CaCO_3$ composite have been

electrospun and have been tested for guided bone regeneration. The assays conducted have shown good osteoblast attachment on these scaffolds [65].

Spasova et al. [66] have successfully electrospun nanofibrous polymer mats of poly(L-lactide) (PLLA)/polyethylene glycol (PEG). The tissue compatibility of the electrospun nanofibrous scaffolds was assessed using osteoblast-like cell line MG-63. It was observed that in long-term cultures, osteoblast-like cells organized in tissue-like structure, indicating that PLLA mixed with hydrophilic PEG is a good candidate for engineering scaffolds.

Li et al. [67] have co-electrospun nanofibrous mats of poly (lactide-*co*-glycolide), gelatin and elastin and the feasibility of this material was tested as scaffolds for bone tissue engineering. Rat bone marrow stromal cells seeded on these scaffolds were found to penetrate into the center of the scaffolds and proliferate immediately after seeding. Scaffolds constructed from blends of natural and synthetic polymers have been suggested to be ideal for tissue engineering. Silk fibroin fibers with an average diameter 700 ± 50 nm have been electrospun and have been tested as scaffolds for human bone marrow stromal cells. The biocompatibility and biodegradable properties of silk protein matrix makes it ideal for tissue engineering [68].

1.3.2 Hydroxyapatite and polymer-hydroxyapatite composites

Synthetic hydroxyapatite (HA) particles, films, coatings and fibers are used extensively in bone tissue engineering applications. It can be synthesized by many wet and dry techniques [69]. These calcium phosphate materials are similar in composition to bone apatite materials and have been found to be osteoconductive. These ceramic materials are therefore used in bone tissue engineering [70]. Nanoscale hydroxyapatite

closely mimics the natural apatite materials found in human bone. Hydroxyapatite has been incorporated in various biodegradable polymers to assess its potential as bone scaffolds

Huang et al. [70] have reported the preparation of nanoscale HA by electrospraying of a nano-HA suspension. An ethanolic suspension of hydroxyapatite was electrospun onto a glass substrate using a ring electrode so as to form a spray rather than a stream of droplets. It has been reported that surface topography of hydroxyapatite both on micro and nanoscale affects cell response. Human osteoblast cells seeded on the electrosprayed substrates have shown good attachment and maintained their morphology with visible filopodia attached to nano-HA relics.

Fibrous structure of hydroxyapatite has been fabricated by electrospinning polyvinyl alcohol with a calcium phosphate based sol. Fibrous network with fiber diameters between 200 and 800 nm was obtained after calcinations at 600 ^{O}C for 6 hours. A non-woven highly porous structure was obtained and it has been reported that the porosity of the fibrous network can be varied by altering the polymer molecular weight and volume fraction of sol. These porous and fibrous networks have been suggested as suitable structures for bone regeneration [69]

Kim et al. [71] have electrospun nanocomposites of hydroxyapatite (HA) and poly(lactic acid) (PLA) for bone regeneration. A uniform dispersion of HA in PLA matrix was obtained by suspending the HA in hydroxysteric acid. Cellular assays conducted on these scaffolds have indicated excellent cell attachment and proliferation and also enhanced expression of alkaline phosphatase. These composite nanofibers have been shown to perform better as a bone generation scaffold in comparison to fibrous mats

fabricated using PLA alone. This was attributed to the uniform distribution of HA in the matrix. Such nanocomposites have been suggested as good materials for three dimensional scaffolds.

Novel bone scaffolding materials have been successfully fabricated by electrospinning polycaprolactone (PCL) containing nanoparticles of HA. The scaffolds exhibited very high tensile strength and showed the highest ALP activity [72]. Biodegradable hollow fibers of poly(DL-lactide-co-glycolide) doped with nanocrystalline hydroxyapatite have been studied as scaffolds for biomimetic bone tissue engineering. These materials have been reported to possess superior bioactivity as a result of hydroxyapatite doping [73].

Silk fibroin fibers have been electrospun with bone morphogenic protein 2 (BMP-2) and nanoparticles of hydroxyapatite (HA) and were used for in vitro bone formation. Human bone marrow derived mesenchymal cells seeded on these scaffolds have shown higher calcium deposition and improved bone formation. This is attributed to the combination of BMP-2 and HA in the matrix [74].

Marques et al. [19] have studied the effect of hydroxyapatite incorporation in various starch based scaffolds. Osteoblast-like cells adhesion/proliferation on these scaffolds was assessed. Incorporation of hydroxyapatite exhibited various effects such as changing the degradation behavior and affecting the surface properties depending on the polymer used.

1.4 Scope of Work

Bone tissue engineering is an emerging field of extensive research. Natural polymers are being studied to find the ideal scaffold material to support bone growth. This work aims to evaluate the potential of a natural polymer and its hybrid with hydroxyapatite particles as bone tissue engineering scaffolds.

Cellulose acetate, a natural polymer has been shown to successfully mimic the extracellular matrix in our earlier work. Cellulose acetate was electrospun to fabricate three dimensional scaffolds with defined shape and complex porous structures to biomimic urinary bladder matrix [35]. It has also been shown to provide good control over scaffold design owing to its low water solubility [19]. Hydroxyapatite, a bioactive material has been used in several works as coatings, films, fibers and additives to support bone growth because of its superior bioactivity and excellent mechanical properties. Nanoscale hydroxyapatite particles closely resemble the natural apatite particles found in bone [69-74].

This work serves to demonstrate the utility of electrospinning as a single-step manufacturing technique for fabricating fibrous scaffolds of cellulose acetate and composites incorporated with nanoscale hydroxyapatite. Cell culture studies and morphological characterization have been performed to demonstrate the potential of these materials as ideal candidates for bone tissue engineering.

1.5 Materials

1.5.1 Cellulose acetate

Cellulose, a most plentiful organic compound, is found in higher plants' cell walls [17]. The derivatives of cellulose such as cellulose viscose, cellulose nitrate, cellulose propionate, etc. have many applications ranging from textile fibers, membranes, tablet coatings, etc.

Cellulose acetate (CA), a cellulose derivative was first produced by Paul Schützenberger in 1865 by heating cotton with acetic anhydride, opening a whole new field for producing cellulose acetate [75]. The structure of cellulose acetate is shown in figure 3.

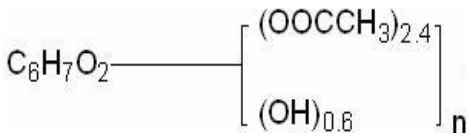

Figure 3 Structure of cellulose acetate (adapted from [76])

CA is soluble in acetone and acetic acid. CA has been previously used to construct scaffolds for functional cardiac cell growth. Scaffolds were constructed by slowly drying the cellulose acetate-acetone solvent mixture. Three dimensional grooved structures were also made by casting the solution into micromachined structures. These scaffolds were found to enhance cardiac cell growth, increase the connectivity of the cells and increase the electrical functionality. These materials have been suggested as ideal candidates because of their versatility and availability [77].

Cellulose acetate (29,000 g/mol) and 40% substitution (acetyl groups) used in our work was purchased from Fluka (Fluka Chemie GmbH CH-9471 Buchs, Switzerland)

1.5.2 Hydroxyapatite

Hydroxyapatite (HA) is chemically similar to the naturally occurring mineral component in bones. It has been used in bone tissue engineering because of its ability to support bone growth and osseointegration. The chemical structure of hydroxyapatite is $Ca_{10}(PO_4)_6(OH)_2$.

Hydroxyapatite particles have shown excellent support for bone growth when used as coating, films, and fibers or in addition with other biodegradable polymers for bone regeneration [69].

1.5.3 Acetone

The chemical formula of acetone is CH_3COCH_3. Figure 4 shows the structure of acetone. Acetone was used as the solvent for cellulose acetate.

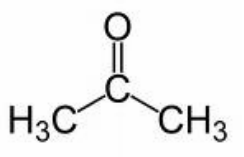

Figure 4 Structure of acetone (adapted from [78])

1.5.4 Acetic acid

The chemical formula is CH_3COOH. Figure 5 shows the chemical structure of acetic acid.

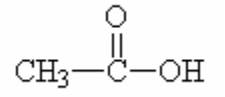

Figure 5 Structure of acetic acid (adapted from [79])

2. EXPERIMENTAL METHODS

2.1 Precursor solution

The precursor solution for CA was made by mixing CA powder (15% w/v) and acetone at room temperature. This solution was sonicated for 1 hour and was used for fabricating fibrous CA scaffolds.

A composition containing 15% w/v of CA and 3.75% w/v of HA nanoparticles (Sigma Aldrich) was mixed in a solvent containing 50:50 (%v) of acetone and acetic acid respectively. The mixture was sonicated for 1 hour to prevent precipitation of CA. This solution was used for fabricating the Cellulose acetate-hydroxyapatite (CA-HA) composite scaffolds.

2.2 Electrospinning conditions

The electrospinning apparatus consists of a high-voltage power supply that can provide as much as 40 kV, with two electrodes, metering pump, a glass syringe with a small diameter needle (millimeter scale) and a collector a metal screen). One of the two electrodes is attached to the needle of the syringe and the other is attached to the collector.

The flow rate was fixed at 160 µl/min and the strength of electric field was fixed at 19 kV for the CA scaffolds while the flow rate was fixed at 41.6 µl/min and the strength of electric field was fixed at 12 kV for the composite scaffolds so as to deposit a single layer of fibrous mat on an aluminum foil. The distance between the tip of the needle and the collector was fixed at 10 cm.

2.3 Characterization of scaffolds

The CA and CA-HA fibrous scaffolds were attached to aluminum stubs and sputter-coated with gold. They were examined under a LEO-Gemini Schottky FEG scanning electron microscope. The working distance used for this study was varied between 8-10 mm and the operating voltage was varied from 5-20 kV. Fiber diameter and pore diameter were determined using ImageJ [78].

2.4 Cell culture and cell seeding

SaOS2 cells were cultured in Dulbecco's modified Eagle's medium (DMEM; Sigma-Aldrich, Milwaukee, USA), supplemented by 10% fetal bovine serum (FBS; Sigma-Aldrich), 1% L-glutamine (Sigma-Aldrich) and 1% antibiotic and antimycotic formulation (Invitrogen Corp., Carlsbad, CA). Cells were incubated at 37^{o}C in a humidified atmosphere containing 5% CO_2. The scaffolds were cut into circular discs about 15mm in diameter. Three scaffolds of each type for each assay were placed in 24-well tissue-culture polystyrene plates (Becton Dickinson, Franklin Lakes, NJ). PTFE rings (McMaster-Carr, Atlanta, GA, part #013TEF) were put on the scaffolds to hold the scaffolds in place in the wells. The disc scaffolds and rings were then sterilized in 70% ethanol for 30 minutes. The scaffolds were then washed with nuclease-free water and immersed in DMEM overnight at 37^{o}C in a humidified atmosphere containing 5% CO_2.

The suspension of cells was seeded in triplicate on CA and CA-HA scaffolds and in empty wells to study cell attachment and proliferation. The seeding density of cells was about 68,000 cells/well for PicoGreen assay and 50,000 cells/well for MTS assay. The cultures were incubated for 1 day and 3 days.

2.5 PicoGreen Assay

The proliferation of cells was determined by quantitation of the double stranded DNA. Quant-iT™ PicoGreen® Kit (Invitrogen) was used to conduct the PicoGreen assay. A DNA standard curve from 1 µg/mL to 50 ng/mL was made. A volume of 100 µL of the Quant-iT™ PicoGreen® reagent was mixed with 100 µL of a series of DNA into 96-well plate (Corning, Corning, NY). The samples were incubated at room temperature for 5 minutes in the dark. After incubation, fluorescence was measured with the excitation wavelength at 488 nm and the emission wavelength at 525 nm using a SpectraMax fluorescence microplate reader. (Molecular Devices, Sunnyvale, CA) [81]. The high-range and low-range standard curves of fluorescence versus DNA concentration are given in figure 6 and figure 7, respectively.

For the attachment study on the scaffolds and controls, after 1 day and 3 days, media was removed from each plate and the scaffold specimens with the rings were moved to empty wells to monitor the difference between the attached cells on the scaffolds and on the plate. Then, 1 mL of 1xTE buffer was added to each well. The plates were sealed and the cells were subjected to two freeze/thaw cycles in order to lyse the cells. Then, 100 µL of the Quant-iT™ PicoGreen® reagent was added to 100 µL of the lysed cells in a 96-well plate. Fluorescence was measured in a fluorescence microplate reader.

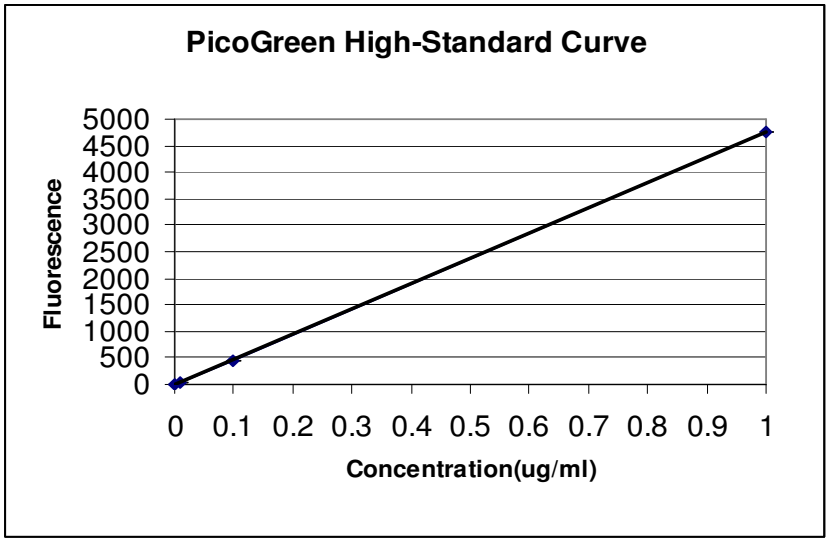

Figure 6 High-range Standard curve of Fluorescence with the excitation wavelength at 488nm and the emission wavelength at 525nm versus DNA concentration between 1µg/mL to 1ng/mL

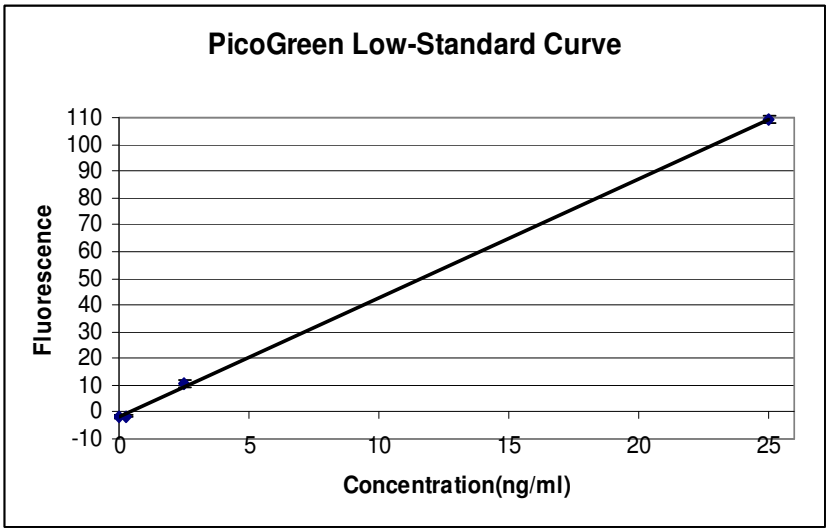

Figure 7 Low-range Standard curve of Fluorescence with the excitation wavelength at 488nm and the emission wavelength at 525nm versus DNA concentration between 25pg/mL to 25 ng/mL

2.6 MTS Assay

The metabolic activity of cells was monitored using a CellTiter 96® Aqueous One Solution Cell Proliferation Assay (MTS) from Promega (Madison, WI). The measurement of the absorbance of the formazan was carried out using 96 well plates after day 1 and day 3 [82].

First, a standard curve for the MTS assay was carried out with a dilution series of cell suspensions from 15.7 cells/mL to 157,000 cells/mL, shown in figure 8. 1.0 mL of each dilution was transferred into wells of a 24-well tissue culture plate in three replicates. Subsequently, 150 µL of the Dye Solution was added to each suspension. The plate was placed at 37C^{o} in a humidified atmosphere containing 5% CO_2 in the dark. After 4 hours, 1.0 mL of Solubilization/Stop Mix was added to each well. Plate was sealed and incubated overnight. Absorbance was read at 570 nm wavelength and also at 650 nm as a reference wavelength using a SpectraMax Spectrophotometer (Molecular Devices).

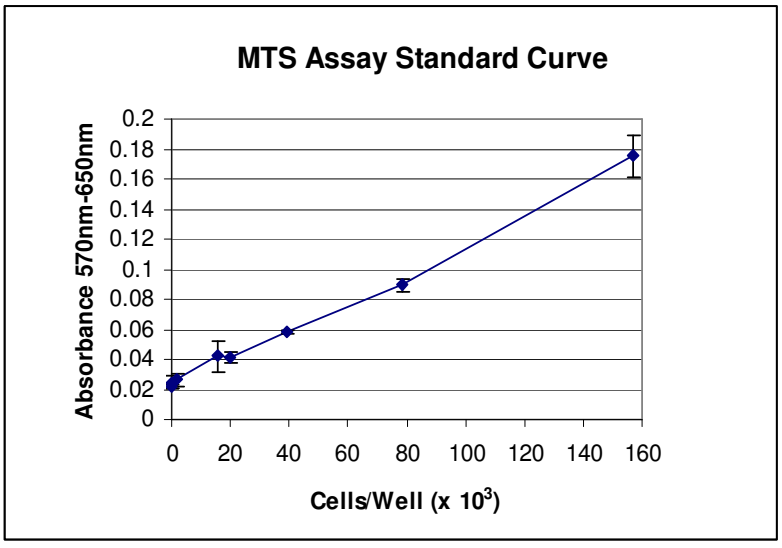

Figure 8 MTS Assay Standard curve of Absorbance at wavelength of 570nm with background subtraction at 650nm versus number of cells

2.7 Morphological Analysis of Cultured Cells

The culture medium was removed from each well at specified times and the cell-cultured CA and CA-HA scaffolds were rinsed twice with PBS (Sigma-Aldrich). The cell-scaffold constructs were fixed in 3% gluteraldehyde solution (Electron Microscopy Science, Hatfield, PA), dehydrated through a graded series of ethanol solutions, 100% Hexamethyldisilazane (HMDS; Sigma) followed by drying in the air [72]. The cell-scaffold constructs were then attached to aluminum stubs and sputter-coated with gold. They were examined under a LEO-Gemini Schottky FEG scanning electron microscope. The working distance used for this study was varied between 8-10 mm and the operating voltage was varied from 5-20 kV.

2.8 Fluorescence microscopy

The samples were dyed with 0.5 µg/ml DAPI/ANTIFADE I solution (Millipore) for 5 minutes. The dye was allowed to spread through the CA and CA-HA cell-scaffold constructs by slightly rocking the samples. They were later washed with PBS buffer solution and were observed under fluorescence microscope with bright field lamp and fluorescent lamp.

3. RESULTS

3.1 Structural characterization

SEM micrographs of electrospun scaffolds revealed that the CA fibers were found to be ribbon shaped. The average width of the ribbons was 3.1 ± 0.5 µm. Their thinner section was 0.8 ± 0.3 µm. The CA-HA hybrid mats consist of fibers with wire-like morphology, of an average diameter of 440 ± 170 nm. The average size of hydroxyapatite nanoclusters in the matrix is 970 ± 650 nm. The pore diameter in the CA scaffold varied between 8-12 µm with a porosity of around 80% and the pore diameter in CA-HA varies between 3-7 µm with porosity relatively lesser than CA scaffolds. Figures 9 (a) and (b) show the electron micrographs of CA scaffolds and figures 10 (a) and (b) show CA-HA scaffolds at different magnifications.

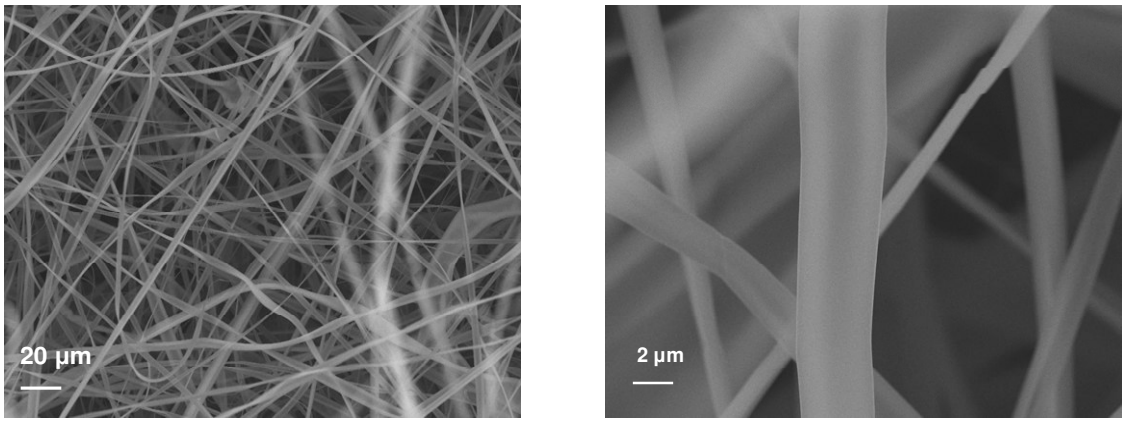

(a) **(b)**

Figure 9 SEM micrographs showing morphology of electrospun fibers **(a)** Morphology CA fibers at 1.5k X **(b)** Magnified image of the fibers at 15k X

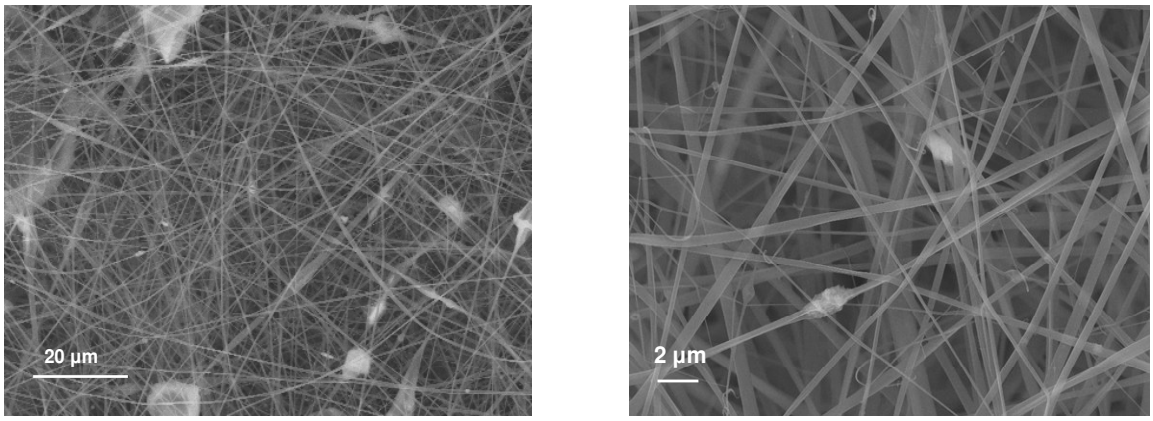

(a) **(b)**

Figure 10 SEM micrographs showing morphology of electrospun CA-HA fibers **(a)** Morphology of the fibers showing hydroxyapatite aggregates at 1.5k X **(b)** Magnified image of the fibers at 15k X

3.2 PicoGreen Assay

Double stranded DNA (dsDNA) in the solution was quantitated by the fluorescence from the PicoGreen assay. The cell proliferation was monitored after 1 day and 3 days (Figure 11). An increase in fluorescence was observed from day 1 to day 3 for CA, CA-HA scaffolds and the control. There was an increase of 48% and 30% for CA and CA-HA scaffolds from day 1 to day 3, respectively while the increase in the control was 25% during this time. Figure 11 shows the fluorescence reading obtained on day 1 and day 3 for all the samples.

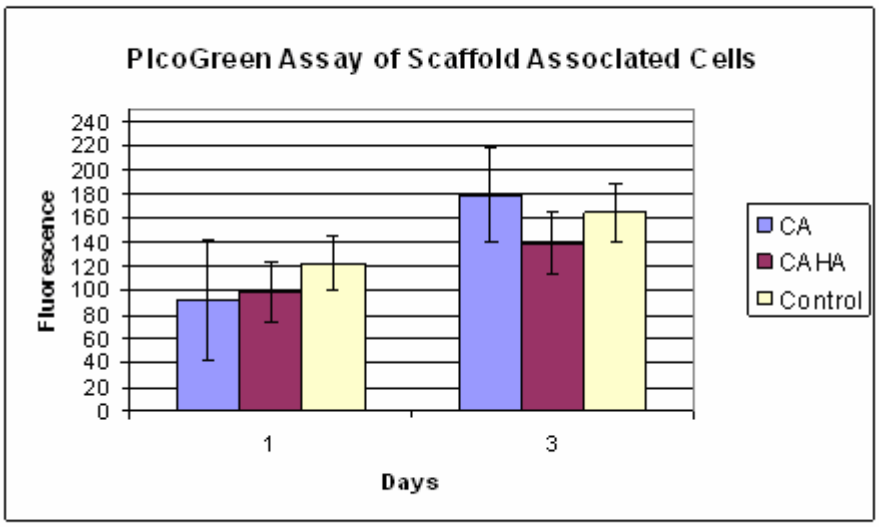

Figure 11 PicoGreen Assay Fluorescence Spectrum after 1 day and 3 days of cells associated with CA and CA-HA scaffolds and Controls. Error bars represent means ±SD

3.3 MTS Assay

MTS is chemically reduced into formazan product, an artificial chromogenic dye formed by the reduction of tetrazolium salts by cells. Since the production of formazan is proportional to the number of living cells, the intensity of the produced color is a good indication of the viability of the cells. The number of cells attached on CA and CA-HA scaffolds is directly proportional to the absorbance reading at 570nm. The metabolic activity of cells was monitored after 1 day and 3 days (Figure 12). There was an increase of 48%, 60%, 113% for CA, CA-HA scaffolds and the control from day 1 to day 3, respectively.

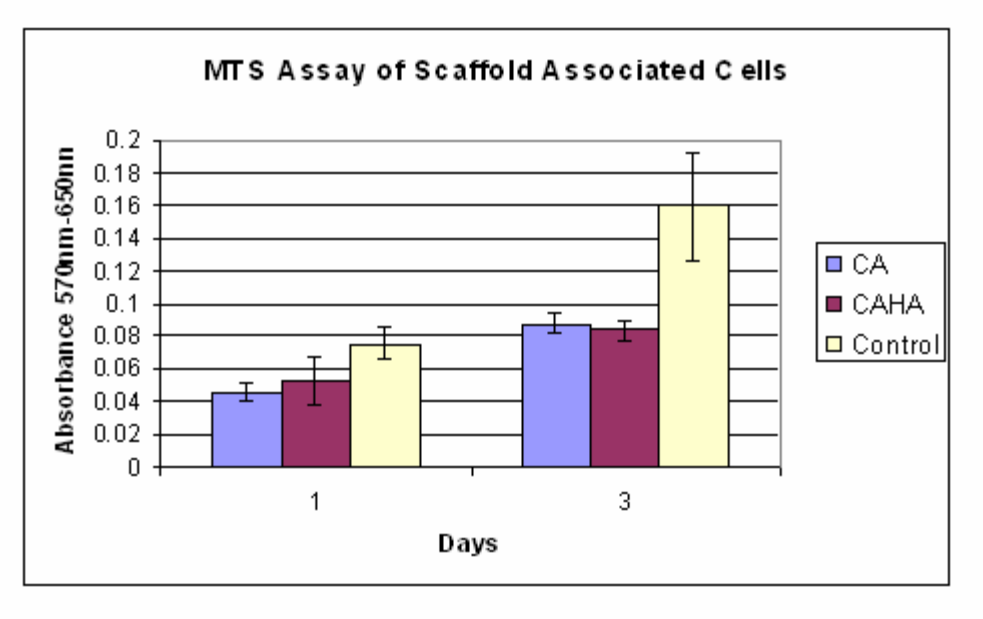

Figure 12 MTS Assay, Absorbance Spectrum after 1 day and 3 days of cells associated with CA and CA-HA scaffolds and Controls. Error bars represent means ±SD

3.4 Morphological Characterization of cell-scaffold constructs

The osteoblasts seeded on the CA scaffold were found to attach along the thinner section of the ribbon-like CA fibers. The cells exhibited a rounded morphology. The average diameter of the cells was 8.5 ± 1.4 µm. The cells were typically found to be attached on a single fiber. Figures 13 (a), (b), and (c) are electron micrographs of different magnification featuring the same cell attached to a single CA fiber.

The osteoblasts seeded on the CA-HA composite scaffolds were attached to several fibers forming an interconnected network. There were only a few cells with rounded morphology. The average diameter of the rounded cells was 6.88 ± 1.53 µm. Figures 14 (a) and (b) are of the same rounded cell that is seen attached to several fibers forming a network, observed at different voltages. In one case, the hydroxyapatite aggregates are clearly shown as bright dots while on the other, a distinct image of how

the cell attaches to the fibers is obtained. The osteoblasts seeded on the CA-HA scaffold however showed mainly a flat morphology. Most of the cells appeared spread out. Figures 15 (a) and (b) show typical images of flat cell spreading, taken at different magnification and using different voltage.

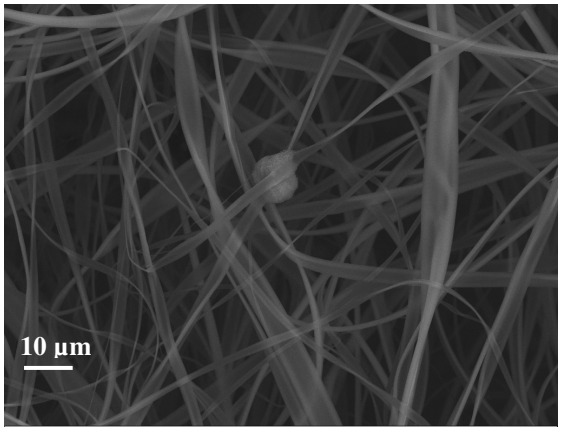

(a)

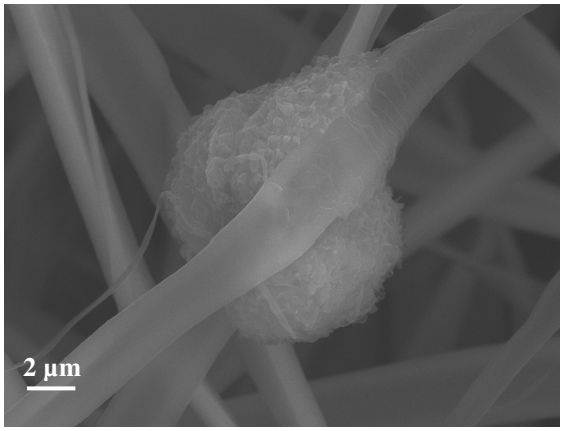

(b)

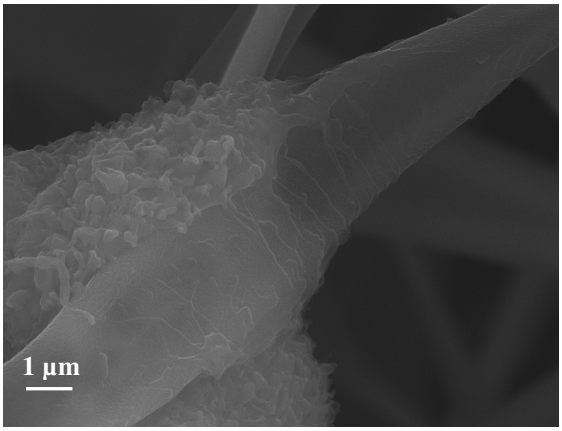

(c)

Figure 13 SEM micrographs showing morphology of an osteoblast attached to CA fiber (day 1 of seeding). **(a)** Morphology of an osteoblast attached to a single CA fiber at 3k X **(b)** Morphology of the same cell at 15k X **(c)** Morphology of the same cell at 30k X; note the stepwise appearance of extracellular matrix products on the fiber

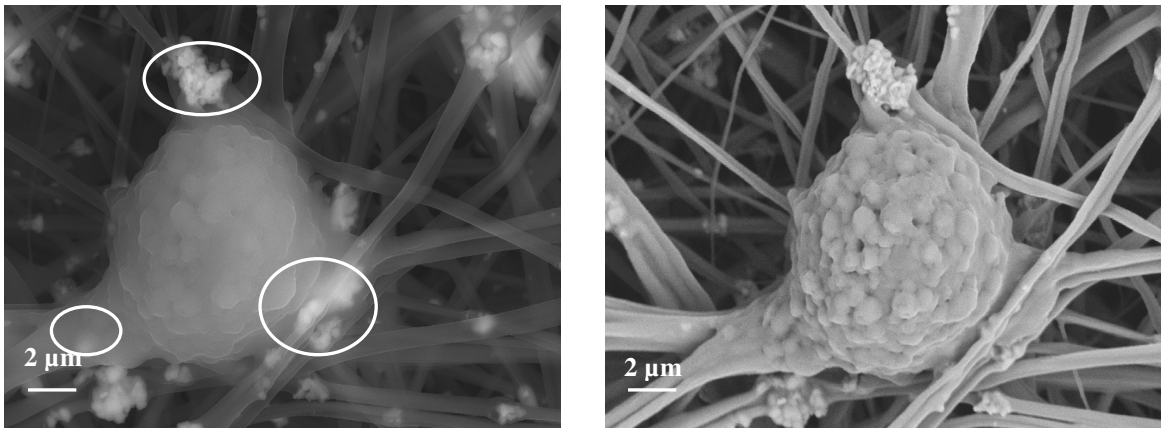

(a) **(b)**

Figure 14 SEM micrographs showing morphology of a osteoblast attached on CA-HA fibers (day 3 of seeding) **(a)** Morphology of a rounded cell at 20k X and 20 kV; circles indicate the presence of hydroxyapatite aggregates at the contact points of the osteoblast. **(b)** Morphology of the same cell at 20k X and 5 kV; image shows how the cell is attached to the fibers

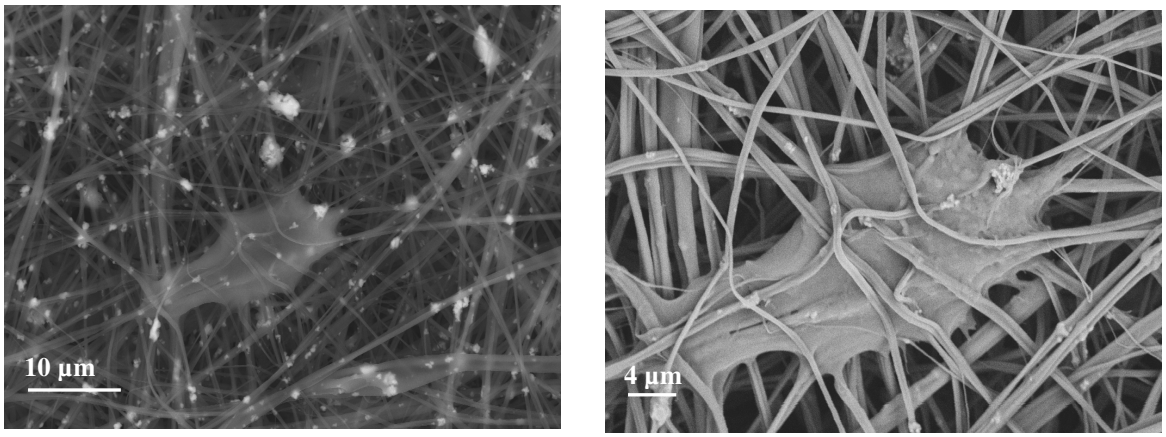

(a) **(b)**

Figure 15 SEM micrographs showing the morphology of a flat and spread out cell attached to CA-HA fiber (day 3). **(a)** At 5k X and 20 kV **(b)** at 10k X and 5 kV, enlarged view of the flat cell elaborating a large number of pseudopodia covering the fine fibers

3.5 Fluorescence microscopy

Figures 16 (a) and (b) are the bright field and fluorescent microscopy images of cells cultured on CA scaffold on day 1, respectively. Figures 17 (a) and (b) are the bright field and fluorescent microscopy images of cells grown on CA-HA scaffold on day 1.

Figures 18 (a) and (b) are the bright field and fluorescent microscopy images of cells grown on CA scaffold on day 3. Figures 19 (a) and (b) are the bright field and fluorescent microscopy images of cells grown on CA-HA scaffold on day 3, respectively.

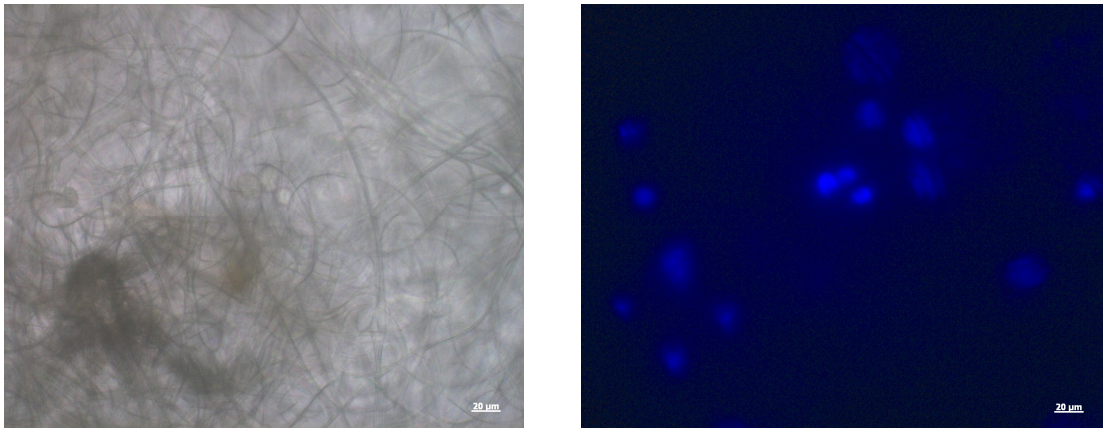

(a) **(b)**

Figure 16 (a) Bright field image of CA scaffold with cell growth on day 1 **(b)** Fluorescent microscopy image of the same (scale 20µm)

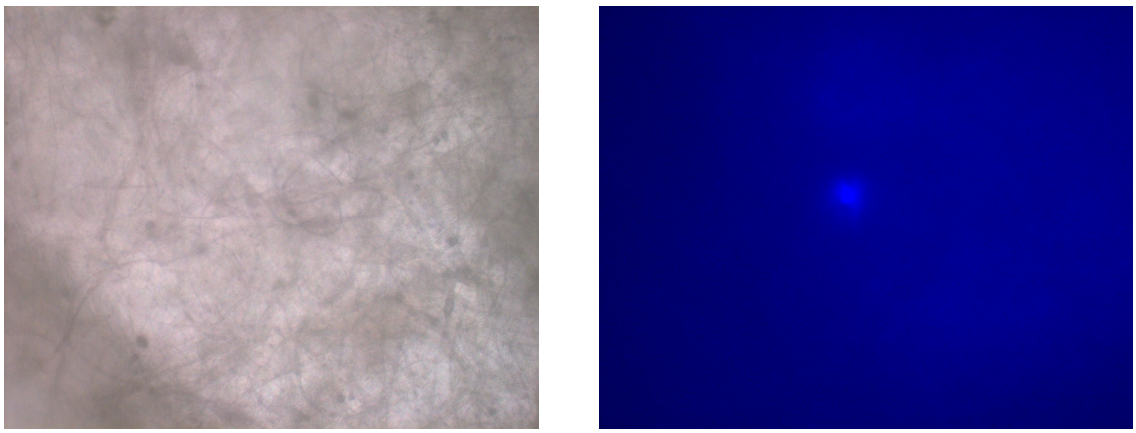

(a) **(b)**

Figure 17 (a) Bright field image of CA-HA scaffold with cell growth on day 1 **(b)** Fluorescent microscopy image of the same (scale: 20µm)

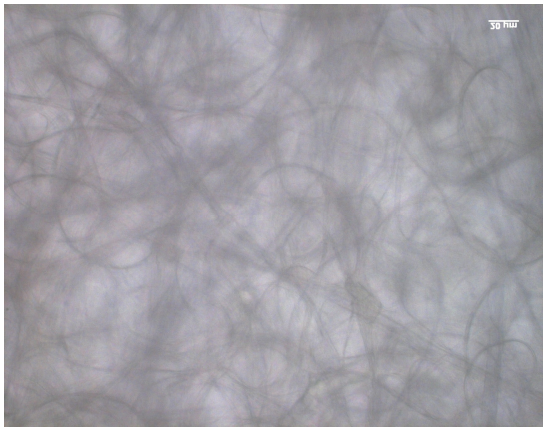

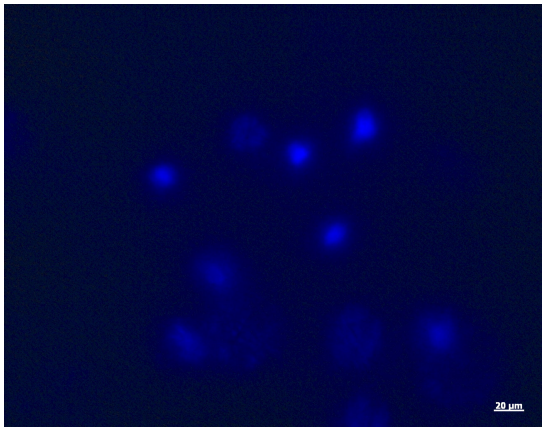

(a) **(b)**

Figure 18 (a) Bright field image of CA scaffold with cell growth on day 3 **(b)** Fluorescent microscopy image of the same (scale: 20µm)

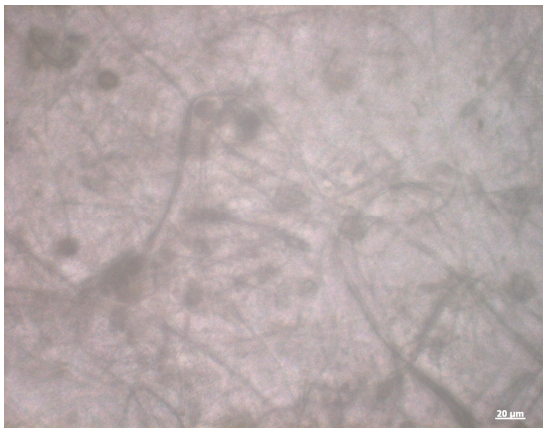

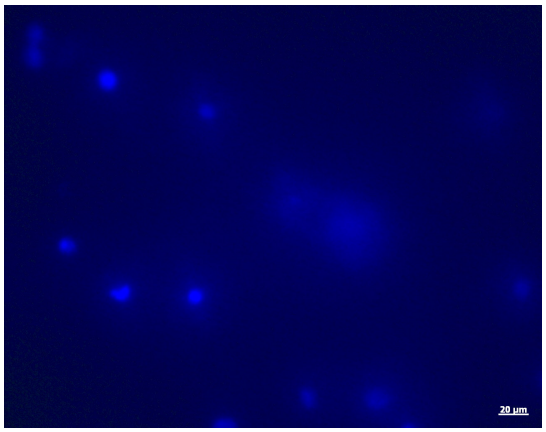

(a) **(b)**

Figure 19 (a) Bright field image of CA-HA scaffold with cell growth on day 3 **(b)** Fluorescent microscopy image of the same (scale: 20µm)

4. DISCUSSION

This study explored the feasibility of CA and CA-HA nanocomposite hybrid mats as potential scaffolds for bone tissue engineering. The MTS assay suggests a significant increase in the number of cells between day 1 and day 3 on both the CA and the CA-HA hybrid scaffolds. Formazan product is formed when MTS is reduced by the cells, this formation of formazan is measured in this assay and the amount of soluble formazan product is directly proportional to the number of live cells in the culture [82]. MTS assay readings suggest a significant increase in the number of live cells. The PicoGreen assay, a quantitative measure of double stranded DNA, is an alternative measure of cell proliferation. This assay also indicated a significant increase in the number of proliferating cells between day 1 and day 3 for both scaffolds. Thus, it is clear that these scaffolds support cell proliferation.

Structural characterization of the CA and CA-HA scaffolds indicate fibrous structures with diameters of a few microns for CA and several nanometers for CA-HA scaffold respectively. Fibrous structures of this nature are ideal as tissue engineering candidates because the small diameter of the fibers provides a high surface area-to-volume ratio for cell attachment and proliferation [7]. The scaffolds reveal a porous structure with varying diameters of interconnected pores throughout the matrix that is ideal for cell growth into the matrix and also for oxygen transport and nutrient delivery [4]. The nanoaggregates of hydroxyapatite particles in the cellulose acetate matrix possess excellent bioactivity and serves to stimulate the cells to undergo the osteoinductive path.

Morphological characterization studies carried out on the cell-scaffold constructs using electron microscopy suggests that the osteoblasts prefer to attach to thinner fibers. It was evident from the fact that the cells seeded on CA scaffolds adhered along the thinner section of the ribbon-like fibers. Cells seeded on CA-HA fibers were observed to attach to multiple fibers elaborating a large number of anchoring ligands. This is related to the fact that the fiber diameter of CA-HA fibers was significantly smaller compared to the CA fibers, thus having a direct influence on the cell attachment behavior. It was clear that hydroxyapatite nanoclusters provided anchoring sites for the cells in the CA-HA mats as observed from the electron micrographs. The cell density was also observed to be higher in the case of CA-HA hybrid mats. Characterization was also carried out using fluorescence microscopy. DAPI, a nucleic acid stain was used to stain the cell-scaffold constructs. The stained samples were observed under bright field and fluorescence light, the blue spots revealed in fluorescence microscopy images correspond to the nuclei of the cells. These corresponded to the location of the cells attached to fibers observed under bright field.

Osteoblasts are anchorage-dependent cells; hence they depend on the high surface area of the scaffolds and the porosity for the attachment and migration of cells in the scaffold [60]. The electrospun CA and CA-HA hybrid scaffolds have fine fiber diameters indicating a high surface area-to-volume ratio suitable for osteoblast attachment and migration. Yoshimo et al. [60] have electrospun microporous, non-woven PCL scaffolds with three-dimensional fibrous mesh consisting of randomly oriented fibers with diameters ranging from 20 nm to 5μm for bone tissue engineering. Mesenchymal stem cell-derived osteoblasts seeded on the scaffolds have been reported to migrate into the

scaffold and produce an extracellular matrix of collagen throughout the scaffold, which was confirmed by histology and immunohistochemistry studies [60]. This is relevant to this study, a prominent step-wise morphology of extracellular matrix agents (possibly type I collagen) secreted by the cells is observed.

Pores in a tissue-engineering scaffold make up the space in which cells reside [60]. Pore properties such as shape, size and volume are key parameters that determine the usefulness of a scaffold. High porosities have been reported to provide more structural space for cell accommodation. For bone regeneration, pore sizes between 100 and 350 μm and porosities of more than 90% are preferred [83]. A stiffness value of -0.41 N/m has been reported for electrospun CA scaffolds with a polymer concentration of 16.5% [84]. This suggests that the electrospun fibrous CA scaffolds are very flexible in nature and the pores can dynamically expand to accommodate cell growth into the scaffold.

One of the most important aspects of a successful scaffold is its capacity for cell attachment and interaction. It has been shown that the degree of cell attachment has a direct influence on cell motility, proliferation rate and control of phenotype [83]. Hunter et al. [83] have shown that one of the main regulators of proliferation in anchorage dependent cells is their shape. Cells in a rounded configuration are reported to divide at lower rates than those flattened and well spread. Cell shape has been shown to have a direct influence on DNA synthesis and growth in non transformed cells. A decrease in DNA synthesis with the change of cell shape towards a spheroidal conformation has also been reported. It is thus understood that a critical cell shape is required in anchorage-dependent cells for controlled growth [85]. In this study, the SaOS2 cells attached on CA fibers show rounded morphology and do not show any spreading, suggesting that these

cells attached on CA may divide at a lower rate. It has also been reported that a biomaterial that does not allow spreading might favor a change of cell phenotype from osteoblast to fibroblast [83]. Hydroxyapatite has been reported to increase the amount of cell spreading when incorporated in starch based polymer scaffolds [19]. This is in agreement with the results obtained in this study. The cells attached to CA-HA hybrid fibers appear flattened and well spread out, and considering relevant literature [83, 84], it is understood that these cells might synthesize more DNA and divide at a higher rate. This suggests that the hydroxyapatite nanoaggregates play an important role in cell spreading and differentiation. It was observed that the composition and topography of CA-HA composites play an important role in determining the morphology of the cells.

5. CONCLUSIONS

Cellulose acetate and hydroxyapatite incorporated cellulose acetate composites were assessed as novel biomaterials for bone tissue engineering scaffolds. Cell culture studies have revealed that osteoblast growth is viable on these scaffolds. Structural characterization studies suggest a difference in osteoblast morphology as they attach on the different scaffolds. Cells on CA scaffold maintained a round morphology with lesser evidence of spreading while those on CA-HA scaffold were mostly flat and well spread out. The latter is due to the fiber size and the presence of HA nanoclusters. We believe that this enhances cell differentiation, thus influencing the functionality of the cells. Novel scaffolds of this type utilizing natural polymer and its nanocomposites with tailored fibrous architectures are demonstrated as promising materials for bone tissue engineering.

6. FUTURE WORK

Future work should focus on evaluating the biodegradability of cellulose acetate and cellulose acetate-hydroxyapatite composite in order to meet the requirements of a bioscaffolds for bone tissue engineering. Effects of fiber diameter and scaffold topography on cell attachment and proliferation behavior must be studied to fabricate fibrous scaffolds according to the design requirements. Hydroxyapatite has been shown to enhance cell spreading and attachment, therefore the effect of concentration of hydroxyapatite may be studied to determine the optimal percentage required for bone growth. Longer term studies could give a better understanding of the benefits and relative performance of the scaffolds for cell growth, metabolism, and differentiation. One might expect to see larger differences in favor of the scaffolds in longer term experiments once the cells had time to exceed the growth area of the plastic control wells. Longer term cell culture under static well and or perfusion culture conditions could provide useful insight. Assays measuring alkaline phosphatase, osteopontin, or osteocalcin secretion would allow us to better characterize the cellular phenotype during longer term studies. Composites comprising of a layered structure of cellulose acetate-hydroxyapatite composite as the bottom layer and a top layer with porous cellulose acetate may be fabricated and its potential as a scaffolds should be assessed.

REFERENCES

1. Langer, R. and Vacanti, J.P. Tissue engineering. Science, 260, 920-926, 1993.

2. Salgado, A.J, Continho, O.P and Reis, R.L. Bone tissue engineering: state of the art and future trends. Macromol Biosci 4, 743 -765, 2004.

3. Yaszemski, M.J., Oldham, J. B., Lu, L. and Currier, B. L. Clinical needs for bone tissue engineering technology. Davis, J.E., ed. Bone Engineering. em squared, Toronto, 2000, pp.541-547.

4. Meijer, G.J., de Bruijn, J.D., Koole, R. and van Blitterswijk C. Cell-based bone tissue engineering. PLoS Med 4, 260-264, 2007.

5. Laurencin, C.T., Ambrosio, A.M.A., Borden, M.D., and Cooper, J.A. Tissue engineering: Orthopedic applications. Annu Rev Biomed Eng 1, 19-46, 1999.

6. Kneser, U., Schaefer, D.J., Munder, B., Klemt, C., Andree, C. and Stark, G.B. Tissue engineering of bone. Minim Invasiv Ther 11, 107-116, 2002.

7. Hutmacher, D.W. Scaffolds in tissue engineering bone and cartilage. Biomaterials 21, 2529-2543, 2000.

8. LeGeros, R.Z. Properties of osteoconductive biomaterials: Calcium phosphates. Clin Orthop Relat R 395, 81-98, 2002.

9. Baksh, D., Davies, J.E. and Kim, S. Three-dimensional matrices of calcium polyphosphates support bone growth in vitro and in vivo. J Mater Sci-Mater M 9, 743-748, 1998.

10. Vacanti, C.A., Bonassar, L.J., Vacanti, M.P., and Shufflebarger, J. Replacement of an avulsed phalanx with tissue-engineered bone. New Eng J Med 344, 1511-1514, 2001.

11. Dong, J.A., Uemura, T., Shirasaki, Y. and Tateishi, T. Promotion of bone formation using highly pure porous beta-TCP combined with bone marrow-derived osteoprogenitor cells. Biomaterials 23, 4493-4502, 2002.

12. Yoshikawa, T., Ohgushi, H., Uemura, T., Nakajima, H., Ichijima, K., Tamai, S., and Tateisi, T. Human marrow cells-derived cultured bone in porous ceramics. Bio-Med Mater Eng 8, 311-320, 1998.

13. Deporter, D.A., Komorin, N., Howley, T.P., Shiga, A., Ghent, A., Hansel, P., and Parisien, K. Reconstituted bovine skin collagen enhances healing of bone wounds in the rat calvaria. Calcified Tissue Int 42, 321-325, 1988.

14. Salgado, A.J., Gomes, M.E., Chou, A., Coutinho, O.P., Reis, R.L. and Hutmacher, D.W. Preliminary study on the adhesion and proliferation of human osteoblasts on starch-based scaffolds. Mat Sci Eng C-Bio S 20, 27-33, 2002.

15. Haisch, A., Loch, A., David, J., Pruss, A., Hansen, R. and Sittinger, M. Preparation of a pure autologous biodegradable fibrin matrix for tissue engineering. Med Biol Eng Comput 38, 686-689, 2000.

16. Chen, L.J. and Wang, M. Production and evaluation of biodegradable composites based on PHB-PHV copolymer. Biomaterials 23, 2631-2639, 2002.

17. Meinel, L., Karageorgiou, V., Fajardo, R., Snyder, B., Shinde-Patil, V., Zichner, L., Kaplan, D., Langer, R. and Vunjak-Novakovic, G. Bone tissue engineering using human mesenchymal stem cells: Effects of scaffold material and medium flow. Ann Biomed Eng 32, 112-122, 2004.

18. Kennedy, J.F., Phillips, G.O., Wedlock, D.J., and Williams, P.A. Cellulose and its derivatives: Chemistry, Biochemistry and Applications. Halsted Press, New York, 1985.

19. Marques, A.P. and Reis, R.L. Hydroxyapatite reinforcement of different starch-based polymers affects osteoblast-like cells adhesion/spreading and proliferation. Mat Sci Eng C-Bio S 25, 215-229, 2005.

20. Mikos, A.G., Thorsen, A.J., Czerwonka, L.A., Bao, Y., Langer, R., Winslow, D.N. and Vacanti, J.P. Preparation and characterization of poly(l-lactic acid) foams. Polymer 35, 1068-1077, 1994.

21. Taboas, J.M., Maddox, R.D., Krebsbach, P.H. and Hollister, S.J. Indirect solid free form fabrication of local and global porous, biomimetic and composite 3D polymer-ceramic scaffolds. Biomaterials 24, 181-194, 2003.

22. Ma, P.X. and Choi, J.W. Biodegradable polymer scaffolds with well-defined interconnected spherical pore network. Tissue Eng 7, 23-33, 2001.

23. Kweon, H., Yoo, M.K., Park, I.K., Kim, T.H., Lee, H.C., Lee, H.S., Oh, J.S., Akaike, T. and Cho, C.S. A novel degradable polycaprolactone networks for tissue engineering. Biomaterials 24, 801-808, 2003.

24. Kohn, J. and Langer, R. Poly(iminocarbonates) as potential biomaterials. Biomaterials 7, 176-182, 1986.

25. Laurencin, C.T., Norman, M.E., Elgendy, H.M., Elamin, S.F., Allcock, H.R., Pucher, S.R. and Ambrosio, A.A. Use of polyphosphazenes for skeletal tissue regeneration. J Biomed Mater Res 27, 963-973, 1993.

26. Ibim, S.E.M., Uhrich, K.E., Attawia, M., Shastri, V.R., El-Amin, S.F., Bronson, R., Langer, R. and Laurencin CT. Preliminary in vivo report on the osteocompatibility of poly(anhydride-co-imides) evaluated in a tibial model. J Biomed Mater Res 43, 374-379, 1998.

27. Holy, C.E., Shoichet, M.S. and Davies, J.E. Engineering three-dimensional bone tissue in vitro using biodegradable scaffolds: Investigating initial cell-seeding density and culture period. J Biomed Mater Res 51, 376-382, 2000.

28. Oh, S.H., Kang, S.G., Kim, E.S., Cho, S.H. and Lee, J.H. Fabrication and characterization of hydrophilic poly(lactic-co-glycolic acid)/poly(vinyl alcohol) blend cell scaffolds by melt-molding particulate-leaching method. Biomaterials 24, 4011-4021, 2003.

29. Mooney, D.J., Baldwin, D.F., Suh, N.P., Vacanti, L.P. and Langer, R. Novel approach to fabricate porous sponges of poly(D,L-lactic-co-glycolic acid) without the use of organic solvents. Biomaterials 17, 1417-1422, 1996.

30. Lee, M., Dunn, J.C.Y. and Wu, B.M. Scaffold fabrication by indirect three-dimensional printing. Biomaterials 26, 4281-4289, 2005.

31. Mao, J.S., Zhao, L.G., Yin, Y.J. and Yao, K.D. Structure and properties of bilayer chitosan-gelatin scaffolds. Biomaterials 24, 1067-1074, 2003.

32. Formhals, A. Process and Apparatus for Preparing Artificial Threads. US patent No. 1,975,504, 1934.

33. Li, W.J., Laurencin, C.T., Caterson, E.J., Tuan, R.S. and Ko, F.K. Electrospun nanofibrous structure: A novel scaffold for tissue engineering. J. Biomed. Mater. Res. 60, 613-621, 2002.

34. Li, M.Y., Mondrinos, M.J., Gandhi, M.R., Ko, F.K., Weiss, A.S., and Lelkes, P.I. Electrospun protein fibers as matrices for tissue engineering. Biomaterials 26, 5999, 2005.

35. Han, D., and Gouma, P.I. Electrospun bioscaffolds that mimic the topology of extracellular matrix. Nanomed-Nanotechnol Biol Med 2, 37-41, 2006.

36. Shin, Y.M., Hohman, M.M., Brenner, M.P., Rutledge, G.C. Experimental characterization of electrospinning: the electrically forced jet and instabilities. Polymer 42, 9955-9967, 2001.

37. Dzenis, Y. Spinning continuous fibers for nanotechnology. Science, 34, 1917-1919, 2004.

38. Zeleny J. The discharge of electricity from pointed conductors differing in size. Phys Rev 25, 0305-0333, 1907.

39. Larrondo, L., Manley, R.S.J. Electrostatic fiber spinning from polymer melts .1. Experimental-observations on fiber formation and properties. J Polym Sci Pol Phys 19, 909-920, 1981.

40. Subbiah, T., Bhat, G.S., Tock, R.W., Pararneswaran, S. and Ramkumar, S.S. Electrospinning of nanofibers. J Appl Polym Sci 96, 557-569, 2005.

41. Reneker, D.H., Yarin, A.L., Fong, H. and Koombhongse, S. Bending instability of electrically charged liquid jets of polymer solutions in electrospinning. J Appl Phys 87, 4531-4547, 2000.

42. Kim, J.S. and Reneker, D.H. Polybenzimidazole nanofiber produced by electrospinning. Polym Eng Sci 39, 849-854, 1999.

43. Hsu, C.M. and Shivkumar, S. Nano-sized beads and porous fiber constructs of poly(epsilon-caprolactone) produced by electrospinning. J Mater Sci 39, 3003-3013, 2004.

44. Doshi, J. and Reneker, D.H. Electrospinning Process And Applications Of Electrospun Fibers. J Electrostat 35, 151-160, 1995.

45. Simons, H.L. U.S. Patent No. 3,280,229 1966.

46. Isakoff, L. US Patent No. 3, 593,074 1971.

47. Fine, J., Passaic, N.J., and Sigismondo, A.T. US Patent No. 4,223,101, 1980.

48. Guignard, C. US Patent No. 4,230,650, 1980.

49. Guignard, C. US Patent No. 4,287,139, 1981.

50. Martin, G.H. and Derek, I. US Patent No. 4,043,331, 1977.

51. Martin, G.H. and Derek, I. US Patent No. 4,044,404, 1977.

52. Bornat, A. US Patent, 4,323,525, 1982.

53. Simm, W.L., Claus, G.O., Bonart, R.B. and Bela, V.F.G. US Patent No. 4,069,026, 1978.

54. Theron, A., Zussman, E. and Yarin, A.L. Electrostatic field-assisted alignment of electrospun nanofibres. Nanotechnol 12, 384-390, 2001.

55. Deitzel, J.M., Kleinmeyer, J., Harris, D. and Tan, N.C.B. The effect of processing variables on the morphology of electrospun nanofibers and textiles. Polymer 42, 261-272 , 2001.

56. Shenoy, S.L., Bates, W.D., Frisch, H.L. and Wnek, G.E. Role of chain entanglements on fiber formation during electrospinning of polymer solutions: good solvent, non-specific polymer-polymer interaction limit. Polymer 46, 3372-3384, 2005.

57. McKee, M.G., Wilkes, G.L., Colby, R.H. and Long, T.E. Correlations of solution rheology with electrospun fiber formation of linear and branched polyesters. Macromolecules 37, 1760-1767, 2004.

58. Mikos, A.G., Bao, Y., Cima, L.G., Ingber, D.E., Vacanti, J. P. and Langer, R. Preparation of poly(glycolic acid) bonded fiber structures for cell attachment and transplantation. J Biomed Mater Res 27, 183-189, 1993.

59. Cima, L. G., Vacanti, J. P., Vacanti, C., Ingber, D., Mooney, D. and Langer, R. J. Tissue engineering by cell transplantation using degradable polymer substrates. J Biomech Eng-T ASME. 113, 143-151, 1991.

60. Shih, Y.R.V., Chen, C.N., Tsai, S.W., Wang, Y.J. and Lee, O.K. Growth of mesenchymal stem cells on electrospun type I collagen nanofibers. Stem Cells 24, 2391-2397, 2006.

61. Kim, H.W., Song, J.H. and Kim, H.E. Bioactive glass nanofiber-collagen nanocomposite as a novel bone regeneration matrix. J Biomed Mater Res A 79, 698-705, 2006.

62. Venugopal, J.R., Zhang, Y.Z. and Ramakrishna, S. In vitro culture of human dermal fibroblasts on electrospun polycaprolactone collagen nanofibrous membrane. Artif Organs 30, 440-446, 2006.

63. Yoshimoto, H., Shin, Y.M., Terai, H., Vacanti, J.P. A biodegradable nanofiber scaffold by electrospinning and its potential for bone tissue engineering. Biomaterials 24, 2077-2082, 2003.

64. Baker, B.M. and Mauck, R.L. The effect of nanofiber alignment on the maturation of engineered meniscus constructs. Biomaterials 28, 1967-1977, 2007.

65. Fujihara, K., Kotaki, M. and Ramakrishna, S. Guided bone regeneration membrane made of polycaprolactone/calcium carbonate composite nano-fibers. Biomaterials 26, 4139-4147, 2005.

66. Spasova, M., Stoilova, O., Manolova, N., Rashkov, I. and Altankov, G. Preparation of PLIA/PEG nanofibers by electrospinning and potential applications. J Bioact Compat Pol 22, 62-76, 2007.

67. Li, M., Mondrinos, M.J., Chen, X., Gandhi, M.R, Ko, F.R. and Lelkes, P.I. Co-electrospun poly(lactide-*co*-glycolide), gelatin, and elastin blends for tissue engineering scaffolds. J Biomed Mater Res A 79A, 963-973, 2006.

68. Jin, H.J., Chen, J.S., Karageorgiou, V., Altman, G.H. and Kaplan, D.L. Human bone marrow stromal cell responses on electrospun silk fibroin mats. Biomaterials 25, 1039-1047, 2004.

69. Dai, X.S. and Shivkumar, S. Electrospinning of hydroxyapatite fibrous mats. Mater Lett 61, 2735-2738, 2007.

70. Huang, J., Jayasinghe, S.N., Best, S.M., Edirisinghe, M.J., Brooks, R.A. and Bonfield, W. Electrospraying of a nano-hydroxyapatite suspension. J Mat Sci 39, 1029-1032, 2004.

71. Kim, H.W., Lee, H.H. and Knowles, J.C. Electrospinning biomedical nanocomposite fibers of hydroxyapaite/poly(lactic acid) for bone regeneration. J Biomed Mater Res A 79, 643-649, 2006.

72. Wutticharoenmongkol, P., Sanchavanakit, N., Pavasant, P., and Supaphol, P. Novel Bone Scaffolds of Electrospun Polycaprolactone Fibers Filled with Nanoparticles. J Nanosci Nanotechno 6, 514-522, 2006.

73. Zhang, N., Nichols, H.L., Tylor, S., and Wen, X.J. Fabrication of nanocrystalline hydroxyapatite doped degradable composite hollow fiber for guided and biomimetic bone tissue engineering. Mat Sci Eng C-Bio S 27, 599-606, 2007.

74. Li, C.M., Vepari, C., Jin, H.J., Kim, H.J. and Kaplan, D.L. Electrospun silk-BMP-2 scaffolds for bone tissue engineering. Biomaterials 27, 3115-3124, 2006.

75. Lepeniotis, S., Feuer, B.I. and Bronk, J.M. Phase systems of starch acetate and cellulose acetate: water. Chemometr Intell Lab 44, 293-306, 1998.

76. http://nexant.ecnext.com/coms2/gi_0255-3045/Acetic-Anhydride-Cellulose-Acetate.html.

77. Entcheva, E., Bien, H., Yin, L., Chung, C.Y., Farell, M., and Kostov, Y. Functional cardiac cell constructs on cellulose-based scaffolding. Biomaterials 25, 5753-5762, 2004.

78. http://commons.wikimedia.org/wiki/Image:Aceton-2.png.

79. http://chemistry.about.com/library/glossary/blacetic.htm.

80. Rasband, W.S. ImageJ, U. S. National Institutes of Health, Bethesda, Maryland, USA, http://rsb.info.nih.gov/ij/, 1997-2007.

81. Quant-iT PicoGreen® dsDNA Reagent, Technical manual, (Invitrogen); available at http://probes.invitrogen.com/media/pis/mp07581.pdf. 2005.

82. Promega CellTiter 96® Non-Radioactive Assay Technical Bulletin, http://www.promega.com/tbs/tb112/tb112.pdf.

83. Hunter, A., Archer, C.W., Walker, P.S. and Blunn, G.W. Attachment and proliferation of osteoblasts and fibroblasts on biomaterials for orthopedic use. Biomaterials 16, 287-295, 1995.

84. Rubenstein, D.A. Development of a Novel Bioassay Chamber to Optimize Autologous Endothelial Cell Viability and Density on Topological and Topographical Substrates. [PhD thesis] Department of Biomedical Engineering, Stony Brook University, NY, 2007.

85. Folkman, J., and Moscona, A. Role of cell shape in growth control. Nature 273, 345-349, 1978.

APPENDIX

PicoGreen Assay

Tables a and b shows the fluorescence readings of the cells that remained on the wells and that were associated with the scaffolds on day 1 and day 3 respectively.

Table a PicoGreen Assay, Day 1 Fluorescence Values (RFU) of cells remained on the wells and associated with scaffolds CA and CA-HA samples. Average Fluorescence values (Avg (RFU)) and Standard Deviations (SD) are given.

Sample	RFU of Cells Remained in the Well	Avg (RFU) of Cells Remained in the Well	SD of Cells Remained in the Well	RFU of Scaffold Associated Cells	Avg (RFU) of Scaffold Associated Cells	SD of Scaffold Associated Cells
CA	68.9 59.2 39.1	55.7	15.2	42.9 88.5 143.9	91.8	50.5
CA-HA	43.1 33.6 47.0	41.3	6.9	103.9 72.3 121.8	99.3	25.1

Table b PicoGreen Assay Day 3 Fluorescence Values (RFU) of cells remained on the wells and associated with scaffolds CA and CA-HA samples. Average Fluorescence values (Avg (RFU)) and Standard Deviations (SD) are given.

Sample	RFU of Cells Remained in the Well	Avg (RFU) of Cells Remained in the Well	SD of Cells Remained in the Well	RFU of Scaffold Associated Cells	Avg (RFU) of Scaffold Associated Cells	SD of Scaffold Associated Cells
CA	116.7 59.0 79.4	85.0	29.2	133.3 202.4 202.1	179.3	39.8
CA-HA	63.9 57.1 125.1	82.0	37.4	126.4 168.0 121.5	138.6	25.5

MTS Assay

Tables c and d shows the absorbance readings for day 1 and day 3, respectively.

Table c MTS Assay, Day 1 Absorbance Values (ABS) at 570nm-650nm of cells remained on the wells and associated with scaffolds CA and CA/HA samples. Average Absorbance values (Avg (RFU)) and Standard Deviations (SD) are given.

Sample	ABS of Cells Remained in the Well	Avg(ABS) of Cells Remained in the Well	SD of Cells Remained in the Well	ABS of Scaffold Associated Cells	Avg(ABS) of Scaffold Associated Cells	SD of Scaffold Associated Cells
CA	0.032 0.029 0.029	0.030	0.0017	0.042 0.046 0.051	0.046	0.0045
CAHA	0.032 0.031 0.029	0.031	0.0015	0.036 0.057 0.064	0.052	0.015

Table d MTS Assay, Day 3 Absorbance Values (ABS) at 570nm-650nm of cells remained on the wells and associated with scaffolds CA and CA/HA samples. Average Absorbance values (Avg (RFU)) and Standard Deviations (SD) are given.

Sample	ABS of Cells Remained in the Well	Avg (ABS) of Cells Remained in the Well	SD of Cells Remained in the Well	ABS of Scaffold Associated Cells	Avg (ABS) of Scaffold Associated Cells	SD of Scaffold Associated Cells
CA	0.031 0.036 0.030	0.032	0.0032	0.092 0.080 0.091	0.088	0.0067
CAHA	0.032 0.034 0.033	0.033	0.001	0.077 0.09 0.083	0.083	0.0065

Electroactive chemo-actuators based on polyaniline-cellulose acetate blends

This work is aimed to study the chemical actuation behavior in polyaniline-cellulose acetate composites.

Experimental methods

Preparation and characterization of polyaniline-cellulose acetate composite films

Polyaniline-emeraldine salt (12 %w/v) was added to a solution containing cellulose acetate (12 %w/v) in acetone. This mixture was sonicated for 2 hours to prevent the precipitation of cellulose acetate. This solvent mixture was cast on a glass substrate and it was allowed to dry for 10 minutes at room temperature. The cast film was peeled off from the glass substrate after drying. The cast films were examined under a LEO-Gemini Schottky FEG scanning electron microscope.

Setup for measuring chemoactuation

A 20ml beaker containing 10 ml of acetone was sealed to saturate the vapors. Thin strip of the polymer (dimensions 25mm x 4mm) was cut from the cast films. This polymer strip was exposed to the vapor through a small hole. The strip was fixed at one end, leaving the other end free to move. This same setup was used with ethanol replacing acetone. The setup is described in figure a. An angular plot was placed behind the beaker to determine the maximum angle of bending.

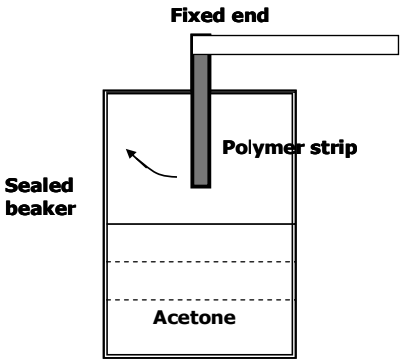

Fig. a Setup for measuring chemical actuation

Results and Discussion

Morphological characterization showed the presence of pores on the surface of the cast films. More pores were found on the surface exposed to the atmosphere than on the surface in contact with the glass substrate. It is believed that there is a gradient in pore distribution in the casting. This causes the bending of the film. As the film adsorbs on the

film, the volume change is higher on the less porous surface, leading to bending towards the more porous surface. Figure b shows a scanning electron micrograph of the surface of the cast film.

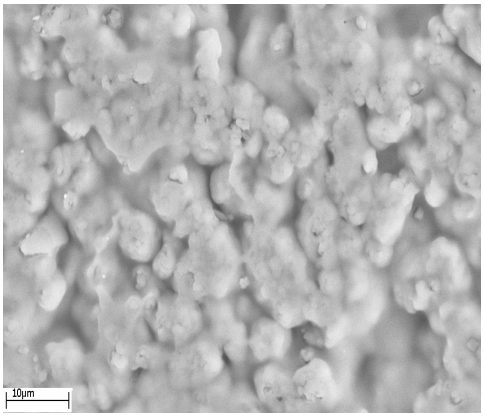

Fig. b SEM image of the surface of the cast film at different magnifications

When the polymer strips were inserted in a beaker containing acetone, the polymer films were observed to show visible bending. The films were observed to bend to a maximum angle of 40 degrees. The maximum bending angle was attained in 4 seconds. When the seal was broken and the polymer film was found to recover to its original configuration in 3 seconds. This kind of bending-recovery was also observed in ethanol; however the bending was not as pronounced as in acetone vapors. This bending-recovery behavior is believed to be caused by the adsorption and desorption of organic vapors. Figure c shows the bending-recovery behavior in acetone.

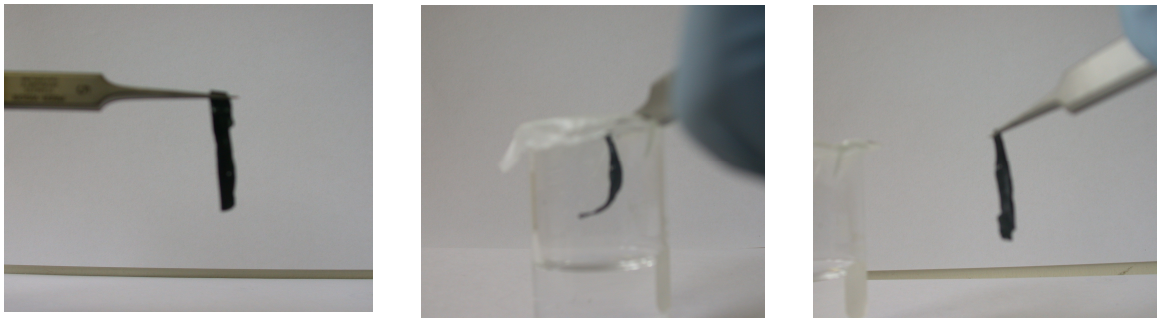

(i) (ii) (iii)

Fig. c Optical images of bending and recovery in polyaniline-cellulose acetate films **(i)** Original configuration **(ii)** Bending in acetone vapors **(iii)** Recovery in air